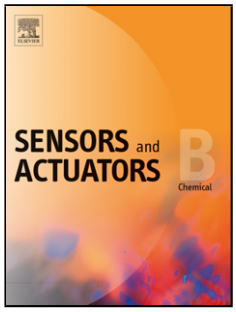

Title: Organic Distributed Feedback Laser to monitor Solvent Extraction upon Thermal Annealing in Solution-processed Polymer Films

Author: Pedro G. Boj Marta Morales-Vidal José M. Villalvilla José A. Quintana Antonio Marcilla María A. Díaz-García

PII: S0925-4005(16)30456-7
DOI: http://dx.doi.org/doi:10.1016/j.snb.2016.03.162
Reference: SNB 19967

To appear in: *Sensors and Actuators B*

Received date: 19-12-2015
Revised date: 9-3-2016
Accepted date: 31-3-2016

Please cite this article as: Pedro G.Boj, Marta Morales-Vidal, José M.Villalvilla, José A.Quintana, Antonio Marcilla, María A.Díaz-García, Organic Distributed Feedback Laser to monitor Solvent Extraction upon Thermal Annealing in Solution-processed Polymer Films, Sensors and Actuators B: Chemical http://dx.doi.org/10.1016/j.snb.2016.03.162

Organic Distributed Feedback Laser to monitor Solvent Extraction upon Thermal Annealing in Solution-processed Polymer Films

Pedro G. Boj[a], Marta Morales-Vidal[b] , José M. Villalvilla[b] , José A. Quintana[a], Antonio Marcilla[c], María A. Díaz-García[b,*]

[a]Dpto. Óptica, Instituto Universitario de Materiales de Alicante y Unidad Asociada UA-CSIC, Universidad de Alicante, 03080 Alicante, Spain.
[b]Dpto. Física Aplicada, Instituto Universitario de Materiales de Alicante y Unidad Asociada UA-CSIC, Universidad de Alicante, 03080 Alicante, Spain.
[c]Dpto. Ingeniería Química, Universidad de Alicante, 03080 Alicante, Spain.

*Corresponding author: Phone: +34 96 590 3543. Fax +34 96 590 9726. Email: maria.diaz@ua.es

ABSTRACT

Solution-processed polymer films are used in multiple technological applications. The presence of residual solvent in the film, as a consequence of the preparation method, affects the material properties, so films are typically subjected to post-deposition thermal annealing treatments aiming at its elimination. Monitoring the amount of solvent eliminated as a function of the annealing parameters is important to design a proper treatment to ensure complete solvent elimination, crucial to obtain reproducible and stable material properties and therefore, device performance. Here we demonstrate, for the first time to our knowledge, the use of an organic distributed feedback (DFB) laser to monitor with high precision the amount of solvent extracted from a spin-coated polymer film as a function of the thermal annealing time. The polymer film of interest, polystyrene in the present work, is doped with a small amount of a laser dye as to constitute the active layer of the laser device and deposited over a reusable DFB resonator. It is shown that solvent elimination translates into shifts in the DFB laser wavelength, as a consequence of changes in film thickness and refractive index. The proposed method is expected to be applicable to other types of annealing treatments, polymer-solvent combinations or film deposition methods, thus constituting a valuable tool to accurately control the quality and reproducibility of solution-processed polymer thin films.

Keywords: solution-process, polymer films, thermal annealing, organic distributed feedback laser

1.-Introduction

Polymer thin films, prepared by solution-based methods such as spin-coating, casting, printing, etc. are used in numerous technological applications. Most of the solvent from the polymer solution evaporates during the deposition process, but a part of it remains in the film, which would affect important properties, such as chain mobility, film homogeneity [1] charge carrier transport [2] or substrate adhesion [3]. Therefore, films are typically subjected, right after deposition, to thermal annealing treatments at a temperature above its glass transition temperature, T_g, aiming at its elimination. Determining a proper treatment to ensure the complete solvent elimination and consequently device reproducibility and stability has been investigated by several authors [1,4,5,6]. The solvent content in thin spin-coated polymer films subjected to thermal treatments has been quantified using techniques such as gas chromatography [4] and neutron reflectometry [5]. The dependency on film thickness of the treatment and the amount of remaining solvent are still a matter of controversy, probably because of differences in the many factors that affect the polymer morphology. For example, the polymer concentration, the type of solvent, the parameters used in the spin coating process, the thermal annealing time and temperature and the adhesion to the substrate surface.

Organic lasers with the active materials in the form of thin waveguide films have received much attention in the last decades due to the advantages of easy processability, chemical versatility, wavelength tunability and low-cost [7,8]. Numerous applications in the fields of spectroscopy, optical communications and sensing have already been demonstrated, most of

them using surface-emitting second-order organic distributed feedback (DFB) lasers [7-9]. The optical feedback in a DFB laser is achieved generally by a relief grating, in most cases patterned over a conventional inorganic substrate by lithographic and etching techniques, over which the active material is coated as a thin film capable of guiding the light along its plane (see Fig. 1). The DFB emission wavelength (λ_{DFB}) appears close to the wavelength at which the cavity resonates (λ_{Bragg}), which is determined by the grating period (Λ), the diffraction order (m) and the effective refractive index (n_{eff}), according to the expression:

$$\lambda_{Bragg} = (2\, n_{eff}\, \Lambda)/m \qquad (1)$$

The n_{eff} parameter depends on the active film thickness (h_f) and on the refractive index of active film, substrate and cover layer (n_f, n_s and n_c, respectively). The principle of operation of previously reported DFB-based bulk refractive index sensors consists on analysing changes in λ_{DFB} upon the deposition over the device of liquid superstrates with different n_c values [10,11]. In comparison to other refractive index sensors, organic DFB lasers are very attractive because of their high sensitivity and resolution, simple fabrication and integration with other devices, wavelength tuning capability and small size. When the DFB laser wants to be used as a biosensor, specificity to a particular analyte is achieved by functionalizing the active film surface as to enable analyte surface binding [12].

In the present work, we report the use of an organic DFB sensor operating differently than the ones just described. Here the DFB laser aims to monitor the extraction of the residual solvent content in polymer films. For that purpose the polymer film of interest is doped with a small amount of an organic laser dye and is deposited over a substrate with a DFB grating, so the polymer film constitutes the organic active layer of a laser device. The polymer used in this study has been polystyrene (PS), which has been the one used in many prior studies aiming to determine the residual solvent content on thermally annealed polymer films. The reported device operates by detecting changes in λ_{DFB} upon n_{eff} variations (see Eq. 1), due to a modification of the active film parameters (h_f and n_f) as a consequence of the solvent extraction upon the thermal treatments. This is in contrast to previously reported DFB laser sensors in which n_{eff} changed because of variations on the superstrate refractive index, while h_f and n_f remained constant. As for the laser dye, we have used a perylenediimide (PDI) derivative, particularly N,N'-Bis(1-hexylheptyl)-perylene-3,4:9,10-bis-(dicarboximide) (PDI-C6) dispersed in PS. PDI-doped PS films have demonstrated a very good performance as active media of organic DFB lasers (low excitation threshold and high photostability) [13,14].

INSERT FIG. 1

The proposed technique has two important characteristics which might be advantageous with respect to other methods to determine refractive index and film thickness. Firstly, it is a simple method for monitoring variations occurring fundamentally in the bulk of the film. Secondly, the wavelength shift determined with the proposed DFB laser sensor is a direct measurement of the effective index, governed by a simple Bragg equation. In this respect, the most classical tool to study surfaces and thin films is ellipsometry, which might have a high sensitivity to detect changes in refractive index, particularly when these occur on the sample surface [15,16]. However, an ellipsometer is in general a relatively complicated instrument.

Besides, it is an indirect technique and information is obtained after analysing data by means of optical models.

2.- Materials and Methods

2.1 Materials

All chemicals were reagent-grade, purchased from commercial sources and used as received. The PDI-C6 dye (molecular weight, M_w = 755, purity higher than 99.5%) was supplied by Phiton. PS and toluene were purchased from Sigma-Aldrich. The PS T_g, measured by differential scanning calorimetry (DSC) with a TA Instruments apparatus, is 65 °C. The PS M_w was determined by a Size Exclusion / Gel permeation Chromatograph (SEC/GPC) apparatus, using three columns: Styragel HR6, Styral HR4 and Styragel HR2. Tetrahydrofuran (THF) was used as eluent at 35 °C. Results have shown that PS consists of a bimodal distribution of two polymers, PS1 and PS2, with M_w values of 72500 and 1300, respectively. By considering the dependence of the PS T_g on molecular weight reported by Blanchard *et al*. [17], and the studies on PS mixtures, according to the Gordon-Taylor equation, performed by Erischen *et al*. [18], the relative composition of the PS used in the present work is estimated as 20 wt.% of PS1 and 80 wt.% of PS2 (details in the supporting information section).

2.2 DFB device preparation and characterization

Active layers with $n_f \sim 1.59$ (at λ = 580 nm) and $h_f \sim 1000$ nm were deposited by spin-coating a toluene solution containing PS, as inert polymer, and 0.5 wt.% of the PDI-C6 laser dye, over a reusable DFB resonator engraved over SiO_2 layers grown on silica plates (more details below). Such low dye concentration was chosen as to avoid perturbations on solvent evaporation, but high enough to have a low laser threshold (1.5 μJ/pulse over an area of 1.0 mm^2) [13]. Additional samples without resonators were prepared by spin-coating PS without PDI-C6 over different substrates as required. Particularly, over transparent fused silica plates (2.5 × 2.5) cm^2 for accurate measurements of thickness and refractive index, or over glass coverslips (2.2 × 2.2) cm^2 for accurate measurements of solvent mass. All samples prepared over fused silica without DFB gratings or over SiO_2 with DFB gratings, constitute waveguides because they comply with the two conditions needed for that purpose. Firstly, n_f is larger than n_s and n_c, whose values are 1.46 and 1, respectively. Note that n_s is the same for both, fused silica and SiO_2; Secondly, h_f is well above the minimum thickness (the so-called cut-off thickness, $h_{cut\text{-}off}$) needed for the propagation of at least one waveguide mode (the transverse electric fundamental mode, TE_0), which for these structures is 150 nm [19]. In fact, these films support, in addition to the TE_0 mode, also the first order mode, TE_1, whose $h_{cut\text{-}off}$ value is 600 nm [19].

Right after films were coated, they were subjected to a thermal annealing in an oven in ambient atmosphere for times, *t*, from 10 min to 24 h. The baking temperature, 90 °C, was chosen as to be near the toluene boiling point (110.6 °C), but not higher, otherwise film quality would decrease due to bubbles formed by the rapid evaporation of the solvent.

The thickness of the annealed active films were measured with high accuracy (error of $\pm$ 2 nm) from the interference pattern of their absorption film spectra [20,21], obtained in a Jasco V-650 spectrophotometer. Their refractive indexes were also determined with high accuracy (error of $\pm$ 0.0005) by means of the Abelès-Brewster-angle method [22,23]. Details of the thickness and refractive index measurement procedures are given in the supporting information section.

The reusable laser resonator consists of a relief grating with size (2 $\times$ 2) mm^2 and period Λ = 368 nm, with equal line and space, and a small depth d $\sim$ 30 nm, engraved on transparent 1.5 µm-thick SiO_2 layers grown by thermal oxidation of silicon wafer plates of size (2.5 $\times$ 2.5) cm^2. The Λ value (368 nm) was chosen to obtain a second order DFB device (m = 2 in Eq. 1), emitting at a wavelength associated with the TE_0 mode and as closest as possible to λ = 579 nm, at which the gain coefficient is maximum. This corresponds to the peak of the amplified spontaneous emission (ASE) spectrum of a 0.5 wt.% PDI-C6-doped PS film. The grating depth was chosen to be small, only a 3% of the active film thickness (hf ~1000 nm) so that grating aspect ratio (0.08) was small enough to guarantee that solvent is not trapped in the surface corrugation. Grating fabrication was accomplished by thermal NIL and subsequent reactive ion etching as described elsewhere [14].

The DFB laser operates under photoexcitation by using a frequency-doubled Nd:YAG laser (10 ns, 10 Hz) emitting at 532 nm. The pump beam is focused to an elliptical spot (area ~1 mm^2) over the sample surface at a 20° angle with respect to the normal to the film. The light emitted by the film is collected perpendicularly with an Ocean Optics MAYA2000 fiber spectrometer with a resolution of 0.07 nm, placed at 1 cm from the sample. All the optical measurements described have been performed in the different samples prepared after annealing, once the samples have been taken out from the oven and cooled down to room temperature, ~22 °C.

2.3 Measurements of solvent loss in the polymer film

The mass of the toluene evaporated, m_L, after different annealing times was determined by using a microbalance Mettler Toledo XS 105 and a thermobalance TGA Netzsh TG 209. Firstly, the toluene residual m_R in each case was obtained by subtracting the masses of the PS and the glass coverslip support from the total mass of the sample. The amount of PS was determined by measuring the weight loss at around 420 °C corresponding to the PS decomposition in the thermobalance [24]. Secondly, the solvent loss m_L was calculated as the difference between m_R values corresponding to the fresh and the annealed sample. The error of m_L was estimated as $\pm$ 5 µg. For samples with a small amount of toluene, a desorption method with a gas chromatograph Agilent 6890N coupled with a mass spectrometer Agilent 5973 was used (see details of procedures in the supporting information section).

3.-Results and discussion

Laser emission spectra for one of the samples after different annealing times, t, are shown in Figure 2a. The laser emission wavelength (λ_{DFB}), which is around 581.5 nm for the fresh sample, blue shifts as t increases. Figure 2b displays λ_{DFB} as a function of t for one sample and

uncertainty is included in the figure as error bars. It can be seen that λ_{DFB} decays rapidly in the first 30 minutes and then it continues decreasing at a slower rate for several hours. The shift observed in λ_{DFB} upon the increase in t is a consequence of the solvent elimination, as shown in Figure 3. The average toluene content in the fresh sample is ~60 μg (6.5 vol %). Half of this content is evaporated in the first 30 min. The other half is evaporated slowly along 6 h until the remaining solvent is very small, 0.3 μg. It is seen that a not negligible amount of toluene, 0.1 μg, remains in the samples after an annealing time of 24 h.

INSERT FIG. 2

INSERT FIG. 3

By combining data from Figures 2b and 3, the DFB wavelength shifts at different annealing times (with respect to the λ_{DFB} value of the fresh sample), denoted as $\lambda_{s\text{-}DFB}$, have been represented in Figure 4 as a function of the m_L. This representation is useful to assess the sensitivity of the laser device used here as a sensor of the amount of solvent eliminated. Two regimes can be distinguished: regime I, with a rate of $\Delta\lambda_{s\text{-}DFB}/\Delta m_L$ ~0.050 nm/μg, during which approximately the first half of the solvent is extracted; and regime II, with a lower rate ($\Delta\lambda_{s\text{-}DFB}/\Delta m_L$ ~0.0075 nm/μg), which corresponds to the slow extraction of the second half of solvent. Note that measurements in the first part of regime I (approximately the first 5 min), are difficult to perform mainly because of temperature variations during the time to reach steady-state inside and outside the oven.

INSERT FIG. 4

The observation of shifts in λ_{DFB} upon solvent elimination is because of changes in the active film thickness (h_f) and refractive index (n_f), as indicated by measurements of these two parameters (see Table I). The average h_f value of the fresh samples is ~ 1000 nm. After 30 min in the oven it quickly decreases down to ~990 nm, a value approximately equal to that obtained with an annealing time longer than two hours. On the other hand, n_f decreases gradually in the range where h_f is constant. Besides, the value after an annealing time of 30 min is approximately equidistant between the average value obtained for the fresh sample, and that corresponding to a sample annealed during 6 h. From these measurements, it can be concluded that the shift $\lambda_{s\text{-}DFB}$ in the regime I is due to variations in both h_f and n_f, although with a stronger contribution of the former. On the other hand, in regime II, h_f is practically invariant with t, while n_f keeps decreasing as in regime I. This explains the higher rate observed in regime I, with respect to that of regime II.

Table 1 includes also theoretical values of the effective index and the laser emission wavelength. The calculated n_{eff} values (n_{eff}^{calc}) were obtained by solving the propagation wave equation for the TE_0 mode, at the wavelength at which laser emission is observed, assuming the simplest possible model waveguide consisting of a film of thickness h_f and refractive index n_f, deposited over a flat substrate (the presence of the grating is neglected) of infinite thickness and with a refractive index value of n_s [14,19,25], being air the cover layer (n_c = 1). Once n_{eff}^{calc} is known, the corresponding λ_{Bragg} value (λ_{Bragg}^{calc}) can be calculated directly from Eq. 1. It can be seen that the experimental and theoretical laser wavelength shift values are in very good agreement (error in λ_{Bragg}^{calc} is ± 0.10 nm).

We have explored the possibility of expressing the sensitivity of our system in the usual units nm/RIU. We found that since the DFB laser detects alterations of both, refractive index and thickness in the bulk of the active layer itself, the effective refractive index (instead of the refractive index) of the guiding layer is the most realistic parameter to measure the sensitivity of the sensor. According to the Bragg equation (Eq. 1), the laser wavelength shift and the effective refractive index are related by

$$\Delta\lambda = - \Lambda\, n_{eff} + \lambda_0 \qquad (2)$$

where $\Delta\lambda = \lambda_0 - \lambda$, and λ_0 is the value corresponding to the fresh sample. In the inset of figure 4, $\Delta\lambda_{DFB}$ has been represented as a function of n_{eff}. Both parameters were calculated from experimental measurements of the thickness and the refractive index of the active layer (see Table 1). The calculated bulk effective index sensitivity, defined here as $S_b = \Delta\lambda/\Delta n_{eff}$ is 0.39 × 10^3 nm/ERIU (ERIU refers to an effective refractive index unit). According to eq. 2, this sensitivity value, expressed in nm/ERIU units, is approximately equal to that of the grating period Λ in nm (ca. 368) for the whole range of refractive index values. However, note that this S_b value cannot be compared to those of the standard sensors because for them, this parameter is obtained by considering changes in n_c, instead of in n_{eff}.

Another important parameter to assess the sensor performance is the limit of detection (LOD), which depends not only on the sensitivity but also on the sensor resolution, *r*. Before determining the *r* value of the present devices, it is first necessary to discuss the most important sources of noise. We recognize three sources, as pointed by Tan *et al.* [26], that can decrease the resolution of DFB laser sensors: (1) Spurious signals: Sometimes we have observed double peaks separated less than 0.5 nm in the emission laser spectrum due to defects in the manufacture of gratings. These defects occur because of minute variations in the grating period and can be detected as changes in the diffraction angle before coating the active layer; (2) Integration time: The signal noise can be decreased by increasing the integration time of the spectrometer. This practice is especially important when the DFB laser is pumped with an energy level near threshold due to instabilities in the pump energy. Wavelength shift measurements reported in this paper were made with integrations times in the range 300-500 ms and pump energies about three times over threshold; (3) Temporal averaging: Time averaging is the usual way to decrease the noise level. It is known that by increasing the number of independent measurements, it is possible to detect changes in the wavelength shift of a DFB laser close to 1 pm. Taking into account these considerations, we have performed additional experiments in order to measure the resolution of our system. By considering the sensor *r* as twice the standard deviation, and then fitting the spectral peaks to a Lorentzian fit [27], an *r* value of 1.6 pm has been calculated from a set of 50 spectra. Finally, the LOD, given by the ratio (r/S_b) was obtained to be $4{\cdot}10^{-6}$ ERIU.

Dye photobleaching is generally other important constraint for organic DFB laser sensors, since dye degradation leads to shifts of the laser wavelength, decrease in the emitted intensity and increase of threshold [27]. However, the laser dye used in the presented system has an outstanding photochemical and thermal stability as previously reported [13,28,29], much superior than other reported laser dyes used for sensing purposes [7,8,11]. Particularly, operational half-lives are of around 3×10^5 pump pulses (more than 8 hours) under an optical

intensity of 4 μJ/pulse (three times above the laser threshold) [13]. Therefore, limitations due to this parameter are not expected for the application proposed.

Qualitatively, the behavior shown in Figure 4 for the toluene extraction upon thermal treatment time in PS films is similar to that observed by other authors with other polymers and/or solvents. For example, Richardson *et al*. [30] reported a rapid film thickness decrease, immediately after deposition, on spin-coated poly(methylmethacrylate) films, followed by a sharp decrease in solvent loss and film thickness decrease after the polymer fraction reached a given value. Other authors have also observed two regimes, similar to the ones observed by us, which were attributed to the formation of a crust [31]. They argued that whilst the polymer remains rubbery, the crust is not yet formed, so the amount of solvent is relatively large, the polymer chains have high mobility and the toluene loss is favored. As a consequence, solvent evaporates quickly at first and slowly when the chain mobility decreases. In our case, the abrupt slope change observed in Fig. 4 after approximately 30 min, may be due to the early drying of the most external part of the active layer (the one in contact with air). This circumstance would form a barrier, which would slow down the extraction of the residual toluene. In the work de Gennes *et al*, [31] a model to explain the formation of a crust of glassy polymer near the surface of a spin casting film when the solvent evaporates was reported. This model, based on a strongly nonlinear solvent volume fraction profile near the surface, describes the overall evaporation process involving first the formation of the crust, and then the growing of the crust until all the film becomes dry. The diffusion coefficient of the solvent was found to be very low in the crust and much higher in the rest of the film where the concentration of the solvent remains comparatively high. According to this, the observation in our films of a very rapid weight loss at the first stages of the drying process, i.e.: during the first 30 minutes at 90 °C in the oven (see Figure 4), might be indicative of the formation of a crust during this time. Another interesting feature is that the film thickness, which significantly decreases during this first period, remains practically constant after the first 30 min. This could also be a consequence of the crust formation. The vitrification described by Richardson *et al*. [30] could be another complementary explanation of the toluene weight loss observed.

From a quantitative point of view, comparisons of results obtained by different authors are difficult because they depend on many factors such as PS molecular weight, film thickness and the variability of baking conditions. Our results have shown that a significant amount of solvent remains in the freshly prepared films, in agreement with other reports [1,4], but in contrast to some studies in which no measurable quantity of toluene was found [5]. Finally, as for the residual solvent removal, we agree with authors that suggest that some solvent is always retained even in completely dried films.

4.- Conclusions

We have reported the use of an organic distributed feedback (DFB) laser to monitor the amount of solvent extracted from a polymer film as a function of the thermal annealing time. The polymer film of interest was doped with a small amount of a laser dye and deposited on a reusable DFB resonator. Thus, we have shown that solvent removal translates into shifts in the DFB laser wavelength as a consequence of changes in film thickness and refractive index. The technique was applied to study the toluene removal from spin-coated PS films after thermal

annealing at 90°C in an oven in ambient atmosphere. Two regimes were distinguished: regime I, during which approximately the first half of the solvent is extracted at a high rate; and regime II, which corresponds to the slow extraction of the second half of solvent. This dynamics is similar to that described by other authors who found that solvent evaporates quickly at first and slowly when the chain mobility in the polymer decreases. In summary, this work proposes a novel method, based on the use of an organic DFB laser, to study with great accuracy the dynamics of solvent removal from solution-processed polymer films. It is expected that the method could be extended to study other types of annealing treatments, polymer-solvent combinations or film deposition methods.

Acknowledgements

The work was supported by the Spanish Government (MINECO) and the European Community (FEDER) through grant no. MAT-2011–28167-C02-01. M.M.-V. has been partly supported by a MINECO FPI fellowship (no. BES-2009-020747). Dr Merino and Dr Retolaza, at Tekniker (Spain), are acknowledged for supplying the NIL fabricated DFB gratings.

Apendix A. Supplementary data

Supplementary data associated with this article can be found.

References

[1] J. Perlich, V. Körstgens, E. Metwalli, L. Schulz, R. Georgi, P. Müller-Buschbaum, Solvent content in thin spin-coated polystyrene homopolymer films, Macromolecules 42 (2009) 337-344.

[2] D. Prime, S. Paul, Electrical and morphological properties of polystyrene thin films for organic electronic applications, Vacuum 84 (2010) 1240-1243.

[3] T. To, H. Wang, A.B. Djurisic, M.H. Xie, W.K. Chang, Z. Xie, C. Wu, S.Y. Tong, Evolution of the surface morphology of thin asymmetric diblock copolymer films, Thin Solid Films 467 (2004) 59-65.

[4] J. García-Turiel, B. Jérôme, Solvent retention in thin polymer films studied by gas chromatography. Colloid Polym. Sci. 285 (2007) 1617-1623.

[5] X. Zhang, K.G. Yager, S. Kang, N.J. Fredin, B. Akgun, S. Satija, J.F. Douglas, A. Karim, R.L. Jones, Solvent retention in thin spin-coated polystyrene and poly(metal methacrylate) homopolymer films studied by neutron reflectometry, Macromolecules 43 (2010) 1117-1123.

[6] Y. Yang, Y. Shi, J. Liu, T.F. Guo, The control of morphology and the morphological dependence of device electrical and optical properties in polymer electronics, in: S. Hotta (Eds.), Electronic and Optical Properties of Conjugated Molecular Systems in Condensed Phases, Research Signpost: Kerala, India, 2003, pp. 307-354.

[7] S. Chénais, S. Forget, Recent advances in solid-state organic lasers, Polym. Int. 61 (2012) 390–406.

[8] C. Grivas, M. Pollnau, Organic solid-state integrated amplifiers and lasers, Laser Photonics Rev. 6 (2012) 419–462.

[9] J. Clark, G. Lanzani, Organic photonics for communications, Nat. Photonics 4 (2010) 438-446.

[10] M. Lu, S.S. Choi, C.J. Wagner, J.G. Eden, B.T. Cunningham, Label free biosensor incorporating a replica-molded, vertically emitting distributed feedback laser, Appl. Phys. Lett. 92 (2008) 261502.

[11] M. Morales-Vidal, P.G. Boj, J.A. Quintana, J.M. Villalvilla, A. Retolaza, S. Merino, M.A. Díaz-García, Distributed feedback lasers based on perylenediimide dyes for label-free refractive index sensing. Sens. Actuators, B: Chem. 220 (2015) 1368-1375.

[12] A. Retolaza, J. Martínez-Perdiguero, S. Merino, M. Morales-Vidal, P.G. Boj, J.A. Quintana, J.M. Villalvilla, M.A. Díaz-García, Organic distributed feedback laser for label-free biosensing of ErbB2 protein biomarker, Sens. Actuators, B: Chem. 223 (2016) 261-265.

[13] V. Navarro-Fuster, E.M. Calzado, P.G. Boj, J.A. Quintana, J.M. Villalvilla, M.A. Díaz-García, V. Trabadelo, A. Juarros, A. Retolaza, S. Merino, Highly photostable organic distributed feedback laser emitting at 573 nm, Appl. Phys. Lett. 97 (2010) 171104.

[14] V. Navarro-Fuster, I. Vragovic, E.M. Calzado, P.G. Boj, J.A. Quintana, J.M. Villalvilla, A. Retolaza, A. Juarros, D. Otaduy, S. Merino, M.A. Díaz-García, Film thickness and grating depth variation in organic second-order distributed feedback lasers, J. Appl. Phys. 112 (2012) 043104.

[15] H. Arwin. Is ellipsometry suitable for sensor applications? Sens. Actuators A 92 (2001) 43-51.

[16] H. Arwin, M. Poksinski, K. Johansen. Enhancement in ellipsometric thin film sensitivity near surface plasmon resonance conditions. Phys. stat. sol. (a) 205 (2008) 817–820.

[17] L.F. Blanchard, J. Hesse, S.L. Malhotra, Effect of Molecular Weight on Glass Transition by Differential Scanning Calorimetry, Can. J. Chem. 52 (1974) 3170-3175.

[18] J. Erichsen, T. Shiferaw, V. Zaporojtchenko, F. Faupel, Surface glass transition in bimodal polystyrene mixtures, Eur. Phys. J. E 24 (2007) 243–246.

[19] E.M. Calzado, M.G. Ramírez, P.G. Boj, M.A. Díaz-García, Thickness dependence of amplified spontaneous emission in low-absorbing organic waveguides, Appl. Opt. 51 (2012) 3287-3293.

[20] R. Swanepoel, Determination of the thickness and optical constants of amorphous silicon, J. Phys. E: Sci. Instrum. 16 (1983) 1214-1222.

[21] R. Swanepoel, Determining refractive index and thickness of thin films from wavelength measurements only, J. Opt. Soc. Am. A 2 (1985) 1339-1343.

[22] F. Abelès, Methods for determining optical parameters of thin films, in: E. Wolf (Eds.), Progress in Optics, North Holland, 1963, Vol. 2, pp. 249-288.

[23] P.C. Logofatu, D. Apostol, V. Damian, I.M. Iordache, M.M. Bojan, R. Müller, Abelès method revisited, Appl. Opt. 45 (2006) 1120-1123.

[24] A. Marcilla, M. Beltrán, Kinetic study of thermal decomposition of polystyrene and polyethylene-vinyl acetate graft polymers by thermogravimetric analysis, Polym Degradat. Stabil. 50 (1995) 117-124.

[25] C.L. Chen, Foundations for Guided-wave Optics; Wiley, New Jersey, 2006.

[26] Y. Tan, A. Chu, M. Lu, B. T. Cunningham. Distributed Feedback Laser Biosensor Noise Reduction. IEEE Sensors J. 13 (2013) 1972-1978.

[27] C. Vannahme, M.C. Leung, F. Richter, C.L.C. Smith, P.G. Hermannsson, A. Kristensen. Nanoimprinted distributed feedback lasers comprising TiO2 thin films: design guidelines for high performance sensing. Laser Photonics Rev. 7 (2013) 1036-1042.

[28] M.G. Ramirez, P.G. Boj, V. Navarro-Fuster, I. Vragovic, J.M. Villalvilla, I. Alonso, V. Trabadelo, S. Merino, M.A. Díaz-García. Efficient organic distributed feedback lasers with imprinted active films. Opt. Express 19 (2011) 22443-22454.

[29] E.M. Calzado, J.M. Villalvilla, P.G. Boj, J.A. Quintana, V. Navarro-Fuster, A. Retolaza, S. Merino, M.A. Díaz-García, Influence of the excitation area on the thresholds of organic second-order distributed feedback lasers, Appl. Phys. Lett. 101 (2012) 223303.

[30] H. Richardson, M. Sferrazza, J.L. Keddie, Influence of the glass transition on solvent loss from spin-cast glassy polymer thin films, Eur. Phys. J. E 12 (2003) 87-91.

[31] P. de Gennes, Solvent evaporation of spin cast films: ”crust” effects. Eur. Phys. J. E 7 (2002) 31-34.

Biographies

Pedro G. Boj obtained the Ph.D. in physics in 1986 in the University of Valencia, in the area of optics in holographic recording materials and holographic optical elements. In 1982 he joined the Holographic Centre of the University of Alicante (UA). In 1985 he became Associate Professor of Optics at the UA, position that holds at present. His research activity evolved from the field of holography to the area of organic solid-state lasers, since 2002, when he joined the group of “Organic Electronics and Photonics” at the UA.

Marta Morales-Vidal received the Optics and Optometry degree in 2007, the Optometry and Vision Sciences Master’s degree in 2009, the Molecular Nanoscience and Nanotechnology Master’s degree in 2012, all of them from Alicante University (UA). She has just obtained the Ph.D. in Nanoscience and Nanotechnology at the UA (December 2015). She is currently working towards a PhD in Nanoscience and Nanotechnology in the UA in the “Organic electronics and photonics” group, with particular emphasis in the study of novel organic

materials for lasing and the application of organic distributed feedback lasers for biosensing applications.

José M. Villalvilla graduated in Chemistry in 1985 in the Autonomous University of Madrid and received the PhD in physics in 1992 from the University of Alicante (UA), working in the area of dry recording in III-V materials with ionic beams**.** After postdoctoral work in Cambridge University, UK, during 1996, he became Associate Professor of Applied Physics at the UA, position that holds at present. In 2002 he joined the group of "Organic Electronics and Photonics". Since then, his research activity has focussed on photoconductive polymers and on the fabrication of organic distributed feedback lasers by holographic lithography.

José A Quintana received the PhD degree in Optics from the University of Alicante (UA), Spain, in 1975. As Associate Professor he taught Solid-state Physics at the University of Valencia, Spain, from 1968 until 1972, and Physics and Optics at the UA, from 1973 until 2008. He conducted research in the area of holography from 1968 until 2000. He joined the "Organic Electronics and Photonics" group at the UA in 2002.

Antonio Marcilla obtained the PhD in Chemistry from the Alicante University in 1982. He is full Professor of Chemical Engineering at the Alicante Polytechnic School, since 1994. He founded the "Polymer Processing and Pyrolysis" research group at the "Chemical Process Engineering" research institute at the University of Alicante. He has worked in different Chemical Engineering topics, such as mass transfer, phase equilibrium, unit operations, polymer processing and pyrolysis, recycling and CO_2 capture, and catalysis. He has lately developed effective catalysts reducing the tobacco smoke toxicity.

María A. Díaz-García received the Ph.D. in Physics in 1995 at the Autonomus University of Madrid, Spain. She was part of the pioneer group of Prof. Heeger (Nobel Prize in Chemistry 2000), at the Univ. of California in Santa Barbara, USA, which discovered stimulated emission in semiconducting polymers in 1996. She joined the faculty of the University of Alicante in 2001, where she founded the "Organic Electronics and Photonics" group, which leads since then. She was appointed full professor in 2010. Her latest research focusses on organic optoelectronic materials and devices, with major emphasis on organic lasers.

FIGURE CAPTIONS

Fig. 1. Schematic representation of the organic DFB laser structure, including the excitation and collection geometry used for laser operation. Parameters n_c, n_f, and n_s are the refractive index of the cover layer (air), organic active film and substrate, respectively; h_f is the active film thickness; Λ and d (d << h_f) are the period and modulation amplitude of the grating, respectively; λ_{DFB} is the wavelength of the emitted laser beam.

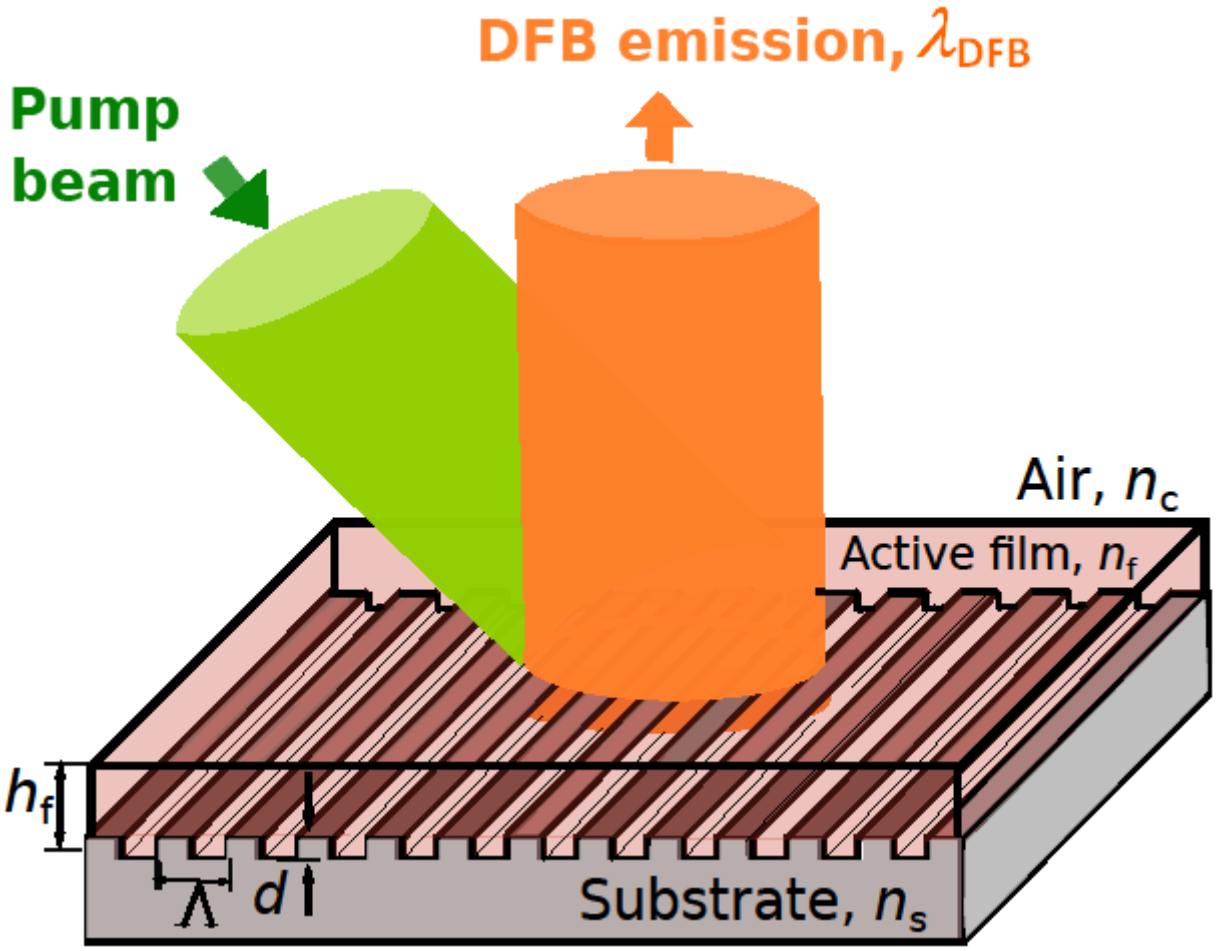

Fig. 2. (a) Laser spectra of a PDI-doped PS DFB laser subjected to thermal treatments in an oven at 90°C at different annealing times, *t* , of 0, 10, 20, 30, 60, 120 and 300 min.; (b) Emission DFB wavelength, λ_{DFB}, versus time, *t*, for the same sample.

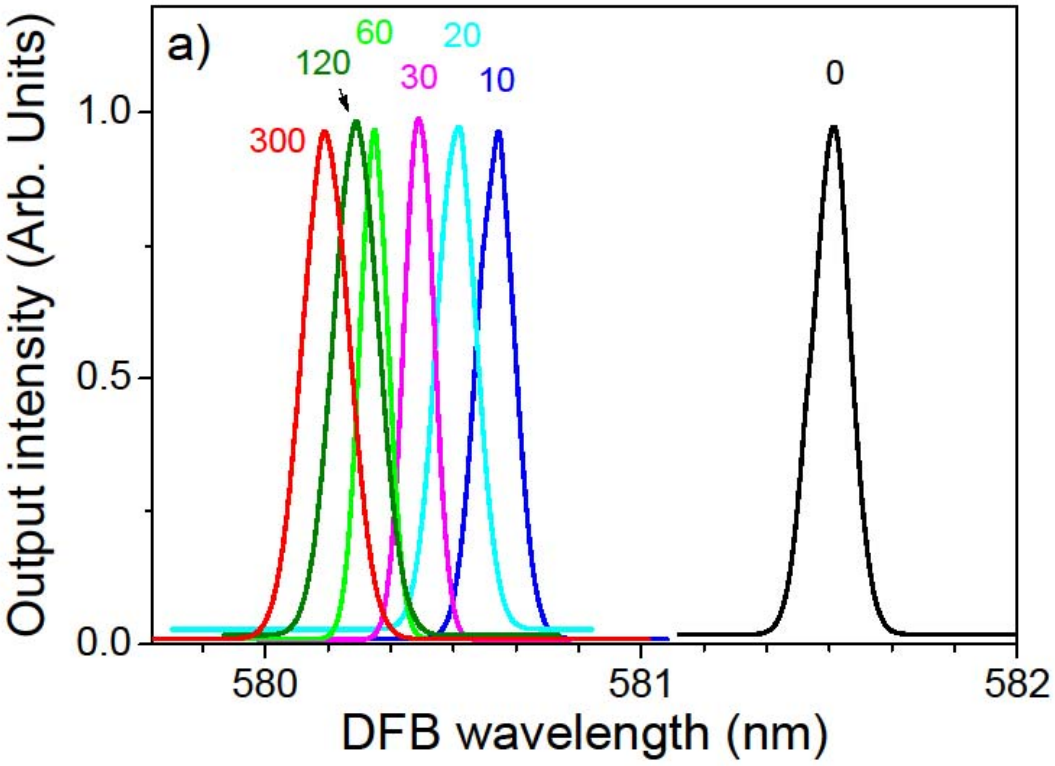

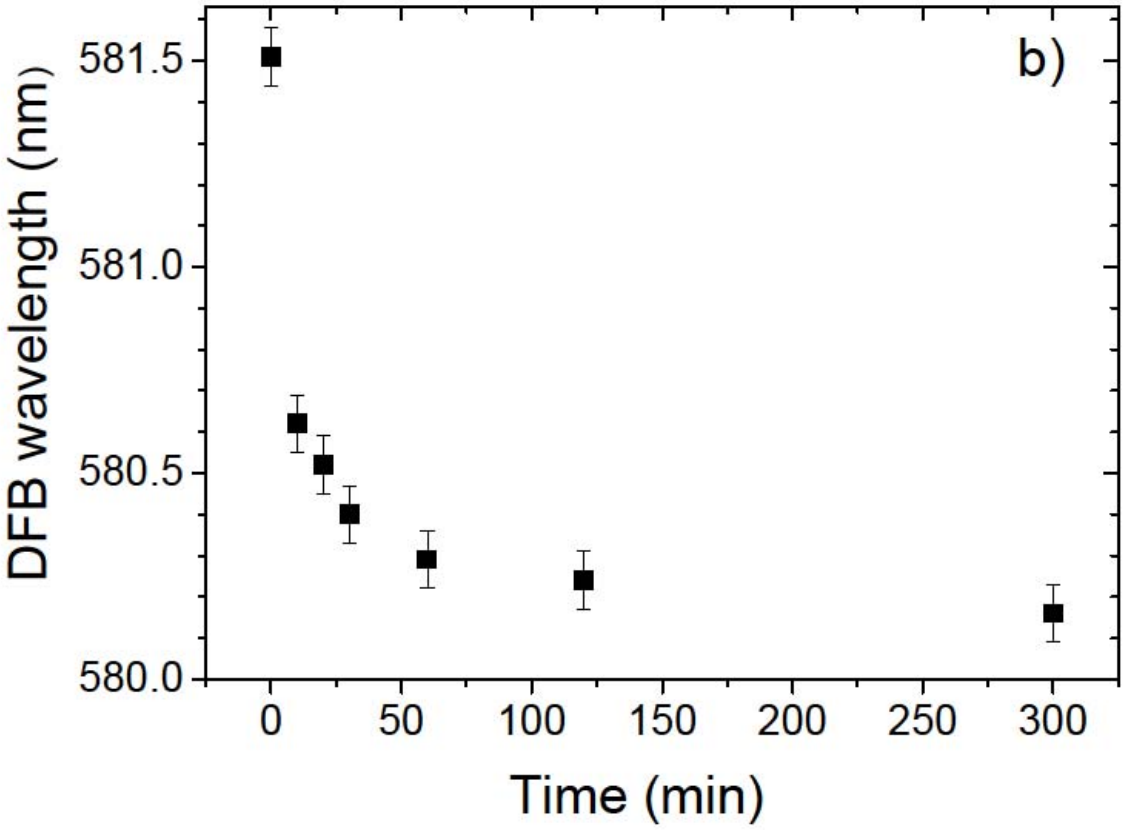

Fig. 3. Residual solvent in the sample, m_R, measured with a microbalance (squares) and with gas chromatography coupled with mass spectrometry (circles), as a function of the annealing time, *t*.

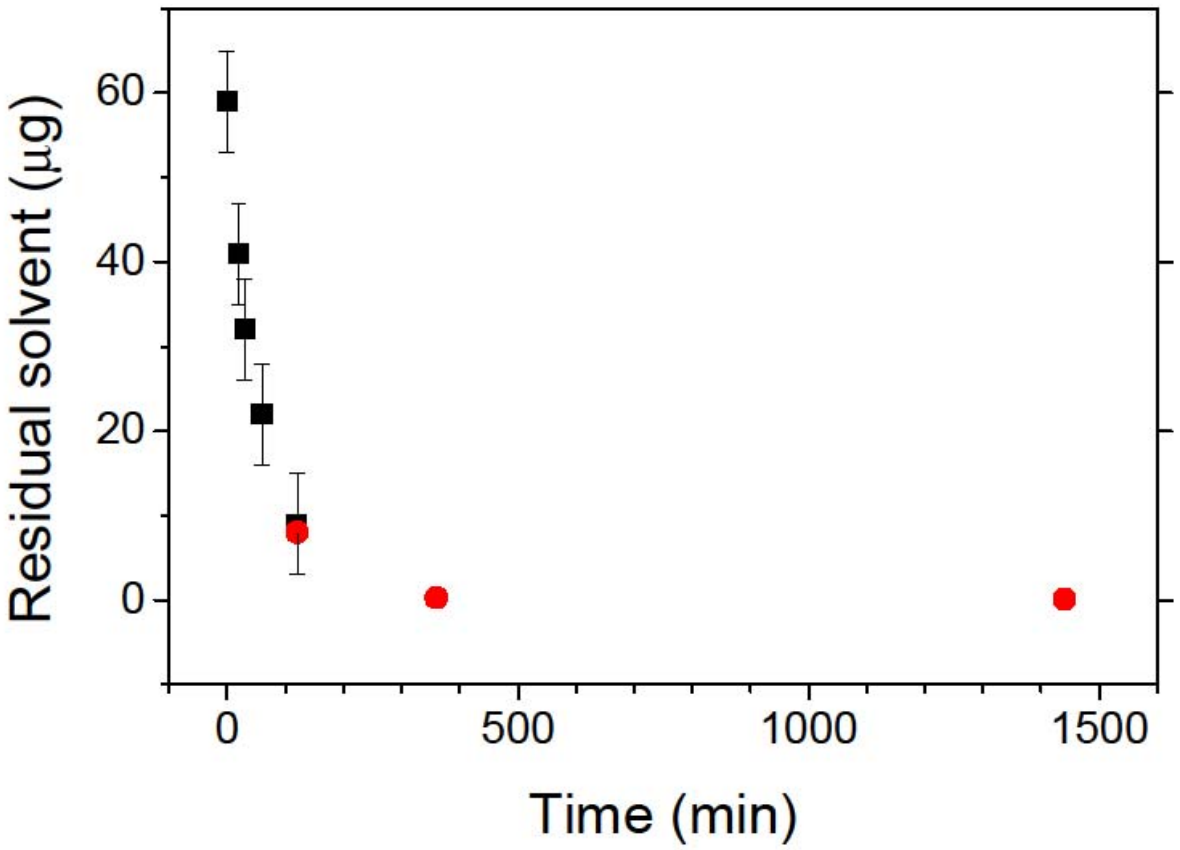

Fig. 4. DFB wavelength shift, $\lambda_{s\text{-}DFB}$, as a function of solvent loss, m_L (both parameters obtained as the difference between the values measured after a given thermal treatment and those of the fresh sample). Dashed lines are guides to the eye. The inset shows $\Delta\lambda_{DFB}$ as a function of n_{eff}, for sensitivity determination purposes.

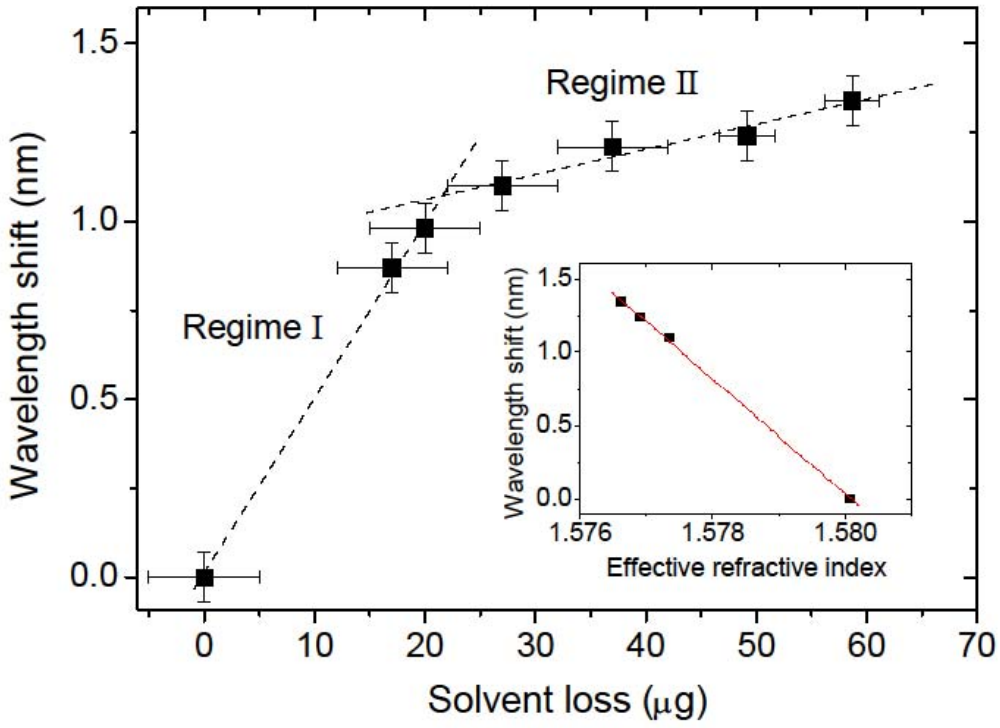

Table 1. Experimental and theoretical laser parameters at different annealing times, *t*.

t (min)	n_f[a]	h_f (nm)[b]	λ_{DFB} (nm)[c]	$\Delta\lambda_{s\text{-}DFB}$ (nm)[d]	n_{eff}^{calc},[e]	λ_{Bragg}^{calc} (nm)[f]	$\Delta\lambda_{Bragg}^{calc}$ (nm)[g]
0 (Fresh sample)	1.5961	1063	581.50	0	1.58007	581.46	0
30	1.5953	992	580.40	1.10	1.57734	580.46	1.00
120	1.5949	991	580.26	1.24	1.57691	580.30	1.16
360	1.5946	991	580.16	1.34	1.57662	580.19	1.27

[a]Active film refractive index. [b]Active film thickness. [c]Experimental DFB wavelength. [d]Experimental DFB wavelength shift. [e]Calculated effective refractive index. [f]Calculated Bragg wavelength. [g]Calculated Bragg wavelength shift.